

Nuclear magnetic resonance on oriented ^{99m}Rh and ^{101m}Rh in Ni

R. Eder,* E. Hagn, and E. Zech

Physik-Department, Technische Universität München, D-8046 Garching, Federal Republic of Germany

(Received 6 November 1989)

With the technique of nuclear magnetic resonance on oriented nuclei, the magnetic hyperfine splitting frequencies $\nu_M = |g\mu_N B_{\text{HF}}/h|$ of ^{99m}Rh ($T_{1/2} = 4.7$ h) and ^{101m}Rh ($T_{1/2} = 4.3$ d) in Ni were determined to be 216.04(10) and 208.68(1) MHz, respectively. The inconsistency of the resonance data of Rh isotopes in Ni in the literature is removed.

I. INTRODUCTION

There have been several unresolved problems in connection with nuclear magnetic resonance on oriented nuclei (NMR-ON) (Ref. 1) experiments on Rh isotopes: (i) The ratios of NMR-ON resonance frequencies of ^{101m}Rh and ^{105}Rh in Fe and Ni were found to be different.² This was unexpected as this ratio represents the ratio of hyperfine fields in Fe and Ni, which should not depend on the isotope. On the other hand, comparing the different hyperfine methods allowing the measurement of the magnetic hyperfine structure, the most precise results are obtained with NMR-ON. This feature is based on the fact that impurity concentrations below the ppm level are sufficient for the detection of the resonance. Thus the inhomogeneous broadening can be reduced to a minimum value, and the resonance frequencies can be determined with an accuracy of 10^{-3} – 10^{-5} . Therefore, it was argued² that the literature value for the hyperfine splitting of $^{101m}\text{RhNi}$, $\nu_M = 207.1(4)$ MHz,³ could be too small by ~ 1.5 MHz. (ii) From the resonance shifts of ^{99m}Rh , ^{101m}Rh , ^{103}Rh , and ^{105}Rh in Fe K values (Knight shift plus diamagnetic shielding) of $-0.048(21)$, $-0.053(11)$, $-0.056(17)$, and $-0.045(13)$ had been determined, yielding an average value of $-0.051(7)$, i.e., statistically significant different from zero.² With Ni as host matrix, resonance shift data are available only for ^{105}Rh , from which $K = -0.02(2)$ had been deduced.⁴ With this value it could not be concluded whether the negative K for Fe is due to a real effect or is introduced spuriously by, e.g., a systematic error of the hyperfine field of Rh in Fe. Thus, additional data on the zero-field hyperfine splitting and the resonance shift of Rh isotopes in Ni were desirable.

II. EXPERIMENTAL DETAILS

Samples of ^{99m}Rh and ^{101m}Rh in Ni were prepared with the recoil-implantation technique. A target stack consisting of 16 ^{104}Pd foils (isotope enrichment 92.7%, thickness 1.0 mg/cm²) and 16 Ni foils (thickness 1.5 mg/cm²; purity > 99.999%) in alternating order was irradiated at the cyclotron in Karlsruhe for 6 h with 100-MeV alpha particles (average current 2.5 μA). ^{99m}Rh and ^{101m}Rh are produced via the compound reactions $^{104}\text{Pd}(\alpha, xny\text{p})$ with $x+y=9$ and 7, respectively. The recoil distance of the

$A=99$ and 101 isotopes with a kinetic energy of ~ 4 MeV is ~ 0.3 μm . Thus all nuclei that are produced in the rear surface layers with a thickness of ~ 0.3 μm are implanted homogeneously into the Ni foils. In addition, several other isotopes produced in the Pd and the Ni foils were observed. Amongst these, ^{52}Mn ($T_{1/2} = 5.7$ d) is well suited for thermometry as the hyperfine splitting and the decay parameters are well known. After the irradiation the most active parts of the Ni foils were soldered to the Cu cold finger of an adiabatic demagnetization cryostat and cooled to 10–15 mK. The γ rays were detected with four $\sim 100\text{-cm}^3$ coaxial Ge(Li) detectors that were placed at 0° , 90° , 180° , and 270° with respect to the external polarizing field B_0 . The rf field was applied perpendicular to B_0 with a one-turn rf coil.

III. RESULTS

After the first demagnetization a final temperature of “only” 15 mK was reached, due to the relatively high activity of short-lived isotopes. The γ anisotropies observed in an external magnetic field $B_0 = 0.96(2)$ kG are listed in Table I. The theoretical description of the anisotropy $A(\theta)$ and the angular distribution $W(\theta)$ of γ radiation is given by

$$A(\theta) = W(\theta) - 1 = \sum_{k=2,4} A_k B_k (h\nu/k_B T) P_k(\cos\theta) Q_k. \quad (1)$$

Here the parameters A_k are products of the normally used angular correlation coefficients F_k and U_k that depend on the specific properties of the nuclear decay chain (spins, multipolarities, and mixing ratios). The parameters B_k describe the degree of orientation; they depend on the sublevel population probabilities a_m . The $P_k(\cos\theta)$ are Legendre polynomials, θ being the angle between the quantization axis—here the direction of the external magnetic field—and the direction of observation, and Q_k are solid-angle correction coefficients. As the independent information of $A(0^\circ)$ and $A(90^\circ)$ is not necessary in NMR-ON experiments, it is more convenient to analyze only the ratio

$$\mathcal{E} = \frac{W(0^\circ)}{W(90^\circ)} - 1, \quad (2)$$

TABLE I. Observed γ anisotropies at $T=15(2)$ mK in an external magnetic field $B_0=0.96(2)$ kG.

Isotope	E (keV)	A (0°)	A (90°)	\mathcal{E}
^{99m}Rh	341	+0.26(2)	-0.15(2)	+0.48(2)
^{101m}Rh	307	+0.37(2)	-0.17(2)	+0.65(2)

as then it is not necessary to correct for the decay due to the finite half-life. The data of Table I show that the γ anisotropy of ^{101m}Rh is $\sim 35\%$ larger than that of ^{99m}Rh . This is due to slightly different $E2/M1$ mixing ratios of the $\frac{7}{2}^+ \rightarrow \frac{5}{2}^+$ γ transitions, as the main branch of the decay cascade is identical for both isotopes, mainly $\frac{9}{2}^+ \xrightarrow{\text{EC}, \beta^+} \frac{7}{2}^+ \xrightarrow{\gamma} \frac{5}{2}^+$. The ratio of \mathcal{E} is 1.35(7), which is in good agreement with the expected value: taking into account the different hyperfine splittings (see further) and the ratio of A_2 coefficients of Ref. 2, we calculate 1.28(5).

In NMR-ON experiments the resonant deorientation of the nuclear-spin system is detected via the destruction of the γ anisotropy. The interaction frequency is given by

$$\begin{aligned} \nu &= \nu_m + |g\mu_N/h|B_0(1+K)\text{sgn}(B_{\text{HF}}), \\ \nu_M &= |g\mu_N B_{\text{HF}}/h|, \end{aligned} \quad (3)$$

where B_0 is the external magnetic field necessary to obtain a macroscopic orientation, ν_M is the usually quoted magnetic hyperfine interaction frequency, g is the nuclear g factor and K is a parameter including Knight shift and diamagnetic shielding.

Starting at 200 MHz, the resonances were searched for $B_0=0.96(2)$ kG with 1 MHz steps and a modulation bandwidth of ± 0.5 MHz. They were found at 215.0(5) MHz (^{99m}Rh) and 207.5(3) MHz (^{101m}Rh).

Next, the ^{99m}Rh NMR-ON resonance was measured for external magnetic fields of 0.96(2), 2.88(6), 4.81(10), and 6.70(13) kG with reduced frequency regions. All measurements were performed with the modulation bandwidth of ± 0.5 MHz and frequency steps of 0.5 MHz. Two resonance spectra are shown in Fig. 1. The results for the resonance centers ν , the linewidths Γ , and the resonance effects I are listed in Table II. The resonance linewidths are rather constant, with an average value 0.82(13) MHz. This is notable, as sometimes an increase of the linewidth with B_0 is observed. Figure 2 shows the resonance centers versus the external magnetic field B_0 . Assuming according to Eq. (3) a linear dependence between ν and B_0 , the least-squares fit yields

$$\nu(B_0=0) = 216.04(10) \text{ MHz},$$

$$d\nu/dB_0 = -0.947(18) \text{ MHz/kG}.$$

After the decay of ^{99m}Rh the NMR resonance of $^{101m}\text{RhNi}$ was measured in detail. Here the measurements could be performed with a modulation bandwidth of ± 0.1 MHz and frequency steps of 0.1 MHz. Resonances measured for 1.92(4), 6.70(13), and 9.56(19) kG are shown in Fig. 3. The resonance centers, the

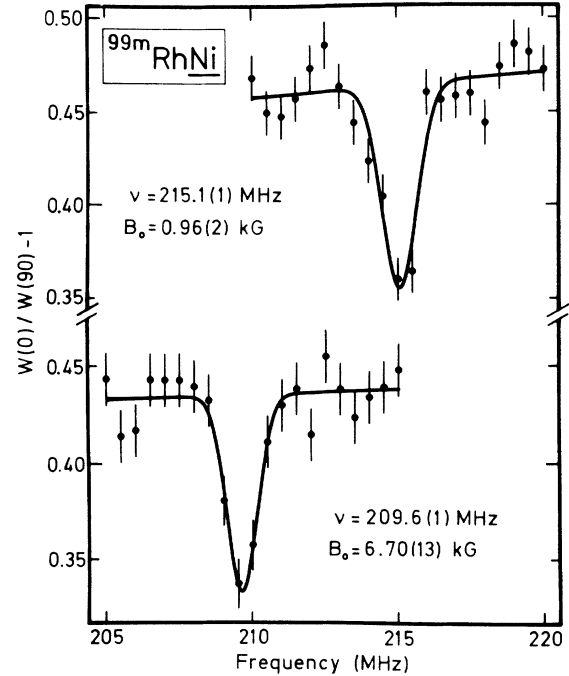


FIG. 1. $^{99m}\text{RhNi}$ NMR-ON resonances of the 341-keV transition measured for $B_0=0.96$ and 6.70 kG. Measurement parameters: modulation bandwidth ± 0.5 MHz; frequency steps 0.5 MHz.

linewidths and the resonance effects are listed in Table II. It is a remarkable fact that the NMR-ON resonance is well observable even for the high external magnetic field of nearly 10 kG. Here again the linewidths show no increasing trend with B_0 . The average value is $\Gamma=0.57(2)$ MHz. The ratio $\Gamma/\nu=2.7 \times 10^{-3}$ indicates a high quality of the used samples. This deserves to be mentioned, especially as the samples were not annealed after the recoil implantation. Figure 4 shows the resonance centers versus B_0 . The least-squares fit yields

$$\nu(B_0=0) = 208.68(1) \text{ MHz},$$

$$d\nu/dB_0 = -0.915(18) \text{ MHz/kG}.$$

Here the main uncertainty in the resonance shift originates from a possible misalignment of the sample and the uncertainty in the calibration of the polarizing magnet. The error of the zero-field splitting contains the uncertainty of the demagnetization factor: For a thin foil with a thickness 1 μm and a diameter of 4 mm the demagnetization field is estimated to be 4 G, corresponding to a frequency shift of 4 kHz in the present case.

IV. DISCUSSION AND CONCLUSIONS

A. Hyperfine interaction aspects

Our zero-field hyperfine splitting for $^{101m}\text{RhNi}$, 208.68(1) MHz, is larger by 1.6 MHz than 207.1(4) MHz of Kaindl *et al.*,³ [In the original paper Kaindl *et al.*

TABLE II. NMR-ON resonance centers ν , linewidths Γ , and resonance effect I of Rh isotopes in Ni measured for different values of the external magnetic field. (For the determination of the linewidths the different modulation bandwidths have been taken into account.)

B_0 (kG)	$^{99m}\text{RhNi}$			$^{101m}\text{RhNi}$		
	ν (MHz)	Γ (MHz)	I (%)	ν (MHz)	Γ (MHz)	I (%)
0.96(2)	215.1(1)	1.0(3)	32(5)	207.79(1)	0.55(2)	96(5)
1.92(4)				206.94(1)	0.59(2)	98(5)
2.88(6)	213.4(1)	0.7(3)	34(5)			
3.85(8)				205.21(1)	0.64(2)	105(5)
4.81(10)	211.6(1)	0.8(2)	28(5)			
6.70(13)	209.6(1)	0.8(3)	24(5)	202.55(1)	0.54(2)	63(5)
9.56(19)				199.91(1)	0.55(2)	49(5)

quote 206.2(4) MHz for an external magnetic field of 1 kG. The extrapolation to zero external magnetic field yields 207.1(4) MHz.] This difference is larger than observed typically in NMR-ON experiments. Its origin is not completely understood at present; it might be because of a larger impurity concentration in the sample used by Kaindl *et al.*, as these authors prepared their sample by deuteron irradiation of natural ruthenium, chemical separation and electroplating of the Rh activity onto a nickel foil. It is easily possible that impurities are introduced during this procedure, and, as known experimentally, impurities may influence the hyperfine interaction considerably. With increasing impurity concentration the linewidth increase in general and the resonance amplitudes decrease. However, the average hyperfine splitting, i.e., the resonance center of NMR-ON resonances, may also be influenced. The linewidth in the experiment of Kaindl *et al.* is considerably larger than those observed in our experiments and the resonance amplitude was only a few percent, i.e., considerably smaller than our amplitudes. As the discrepancy in the ratio of the hyperfine interaction frequencies is removed with our value for the hyperfine splitting of $^{101m}\text{RhNi}$ (see further), we conclude that the result of Kaindl *et al.* is erroneous, most probably because of a too high concentration of impurities in their sample.

The adopted values for the hyperfine splitting frequencies of Rh isotopes in Fe and Ni are listed in Table III,

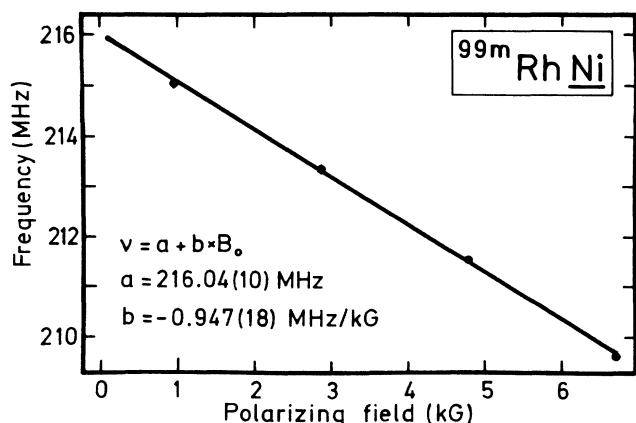


FIG. 2. $^{99m}\text{RhNi}$ resonance shift with the external magnetic field B_0 .

together with the respective ratio in Fe and Ni. This ratio represents the ratio of the hyperfine fields in Fe and Ni and must thus be independent of the isotope. The double ratio

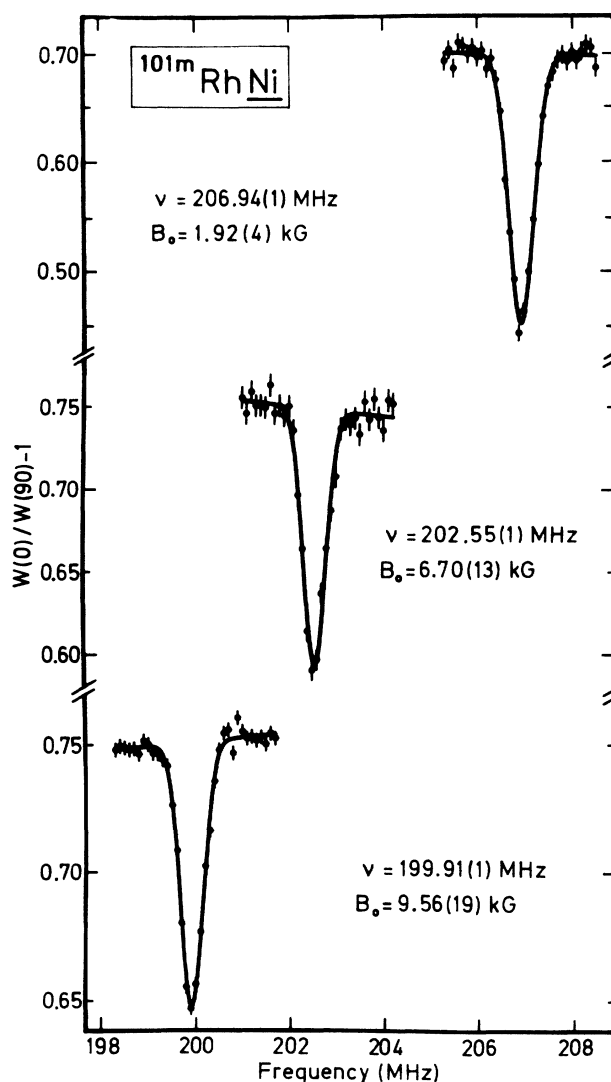


FIG. 3. $^{101m}\text{RhNi}$ NMR-ON resonances of the 306-keV transition measured for $B_0 = 1.92, 6.70,$ and 9.56 kG. Measurement parameters: modulation bandwidth ± 0.1 MHz; frequency steps 0.1 MHz.

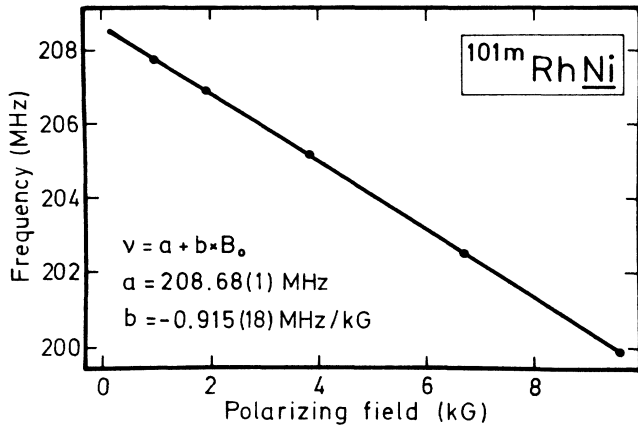


FIG. 4. $^{101m}\text{RhNi}$ resonance shift with the external magnetic field B_0 .

$$xR^y = \frac{\nu_M(^x\text{RhFe})/\nu_M(^x\text{RhNi})}{\nu_M(^y\text{RhFe})/\nu_M(^y\text{RhNi})} \quad (4)$$

should have a nominal value of 1.0. The results are $^{99m}\text{Rh} \ ^{101m}\text{Rh} = 1.0000(5)$ and $^{105}\text{Rh} \ ^{101m}\text{Rh} = 1.0006(3)$. The large discrepancy reported in Ref. 2 is thus removed. The small deviation of $^{105}\text{Rh} \ ^{101m}\text{Rh}$ from 1.0 may be due to a concentration dependency of the hyperfine field as the $^{105}\text{RhFe}$ and $^{105}\text{RhNi}$ samples used by Hagn *et al.*⁴ were prepared by neutron irradiation of $^{104}\text{RuFe}$ and $^{104}\text{RuNi}$ alloys that contained 0.1 at. % Ru. Although the dilute-impurity limit should already be reached at the impurity level of 0.1 at. %, a (small) concentration dependence of the hyperfine field of RhFe or RhNi cannot be excluded. As the deviation on the level of 10^{-4} is only twice the statistical error it should not be overinterpreted.

B. Resonance linewidths and resonance effects

The average value for the linewidth is 0.82(13) MHz and 0.57(2) MHz for $^{99m}\text{RhNi}$ and $^{101m}\text{RhNi}$, respectively. The ratio is 1.44(23), i.e., significantly larger than expected from the ratio of the hyperfine splitting frequencies, which is 1.0353(5). The difference of these ratios is not understood; it may originate from the following different effects.

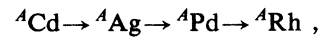
(1) The (total) inhomogeneous linewidth is composed of a magnetic and a quadrupolar part. The “magnetic” inhomogeneous linewidth originates from the inhomogeneous distribution of the hyperfine field; this contribution should scale with the hyperfine splitting frequency. The “quadrupolar” inhomogeneous linewidth originates from

TABLE III. Magnetic hyperfine splitting frequencies of Rh isotopes in Fe and Ni.

Isotope	$\nu_M^{(\text{Fe})}$ (MHz)	$\nu_M^{(\text{Ni})}$ (MHz)	$\nu_M^{(\text{Fe})}/\nu_M^{(\text{Ni})}$
^{99m}Rh	534.28(5)	216.04(10)	2.4731(12)
^{101m}Rh	516.10(5)	208.68(1)	2.4732(3)
^{105}Rh	539.63(3)	218.06(5)	2.4746(6)

the interaction of the nuclear quadrupole moment with randomly distributed electric-field gradients introduced by the distortion of the (cubic) lattice by impurities or radiation-induced vacancies, which were not healed out during the irradiation. Thus a larger linewidth of ^{99m}Rh than expected from the scaling according to the hyperfine splitting frequencies would imply a considerably larger quadrupole moment of ^{99m}Rh in comparison to ^{101m}Rh . Taking into account known facts concerning the nuclear structure of these isotopes, this can be excluded with high confidence.

(2) In principle, different linewidths and resonance effects (see further) for ^{99m}Rh and ^{101m}Rh could be related to the different production and “history” (in the sample). Both isotopes were produced via $(\alpha, xnyp)$ reactions and the chain



with different relative production rates via Cd, Ag, and Pd. Moreover, the Pd precursors ^{99}Pd and ^{101}Pd have half-lives of 21 m and 8.5 h. This means that a large fraction of ^{101m}Rh is produced after the irradiation, whereas ^{99m}Rh is produced mainly during the irradiation. Because of the higher temperature of the foils during the irradiation and the fact that the systems PdNi and RhNi have probably different implantation and annealing properties, the RhNi properties may be more relevant for ^{99m}Rh , whereas the PdNi properties may be more relevant for ^{101m}Rh . The fact that the linewidth may be “history dependent” has actually been observed already with NMR-ON on $^{175}\text{HfFe}$. Samples in which ^{175}Hf was produced *in situ* via the decay of ^{175}Ta showed smaller linewidths than samples in which ^{175}Hf was implanted directly. This fact was explained as being due to the different metallurgical properties of TaFe and HfFe alloys.⁵

Let us now discuss the resonance effects, which are listed in Table II. In most NMR-ON experiments the observed resonance effect is correlated with the linewidth. This is due to the fact that the rf power that can be applied at mK temperatures is always limited by the cooling power of the cryostat and the heat impedance between the cooling stage and the sample. Because of the inhomogeneous linewidth the rf field has to be frequency modulated. Thus the rf power density depends directly on the frequency modulation bandwidth. For the total deorientation of the spin system a minimum rf power density (depending on the strength of the spin-lattice coupling, i.e., the Korringa constant) is necessary, implying a “critical” (upper) value for the modulation bandwidth. This “critical” modulation bandwidth depends also on the external magnetic field via the enhancement factor for the rf field. From measurements of the resonance effect of ^{101m}Rh at $B_0 = 1$ kG with different modulation bandwidths, we estimated the “critical” modulation bandwidth (for $B_0 = 1$ kG) to be ~ 0.3 MHz. In this way, the decrease of the resonance effects of ^{101m}Rh for $B_0 > 4$ kG can be understood as being due to the decreasing enhancement factor. The smaller resonance effects of ^{99m}Rh are due to the larger modulation bandwidth necessary because of the

TABLE IV. Resonance shift parameters $b = d\nu/dB_0$ for Fe and Ni hosts and ratios of the resonance shift parameters. The smaller errors of the ratios are due to the fact that errors of b contain the uncertainty of the calibration of the polarizing magnet, which cancels out in the ratios.

Isotope	$b^{(\text{Fe})}$ (MHz/kG)	$b^{(\text{Ni})}$ (MHz/kG)	$b^{(\text{Fe})}/b^{(\text{Ni})}$
^{99m}Rh	$-0.914(20)^a$	$-0.947(18)$	0.965(28)
^{101m}Rh	$-0.878(10)^a$	$-0.915(3)$	0.960(11)
^{105}Rh	$-0.926(13)^b$	$-0.951(19)$	0.974(24)
average			0.963(9)

^aReference 2.

^bReference 4.

large inhomogeneous linewidth. Thus, the experimental linewidths and the resonance effects are consistent; there is a strong evidence that the distortion of the surroundings of ^{99m}Rh and ^{101m}Rh is slightly different, probably due to the different "history" of both isotopes.

C. Resonance shift aspects

According to Eq. (3) the measurement of the resonance as a function of the external magnetic field B_0 yields $g(1+K)$. As the g factor can in general be determined more precisely from the zero-field hyperfine splitting—most hyperfine fields are now known with high precision—the resonance shift yields information on K . For ^{105}Rh in Fe and Ni it had already been reported⁶ that the K_{Fe} value differed from zero with statistical significance, while K_{Ni} was consistent with zero,

$K_{\text{Fe}} = -0.05(2)$, $K_{\text{Ni}} = -0.02(2)$.⁴ Negative K values for Fe have meanwhile also been reported for ^{103m}Rh (Ref. 7; see discussion in Ref. 2) and $^{99m,101m}\text{Rh}$ (Ref. 2), with an average K value of $-0.051(7)$. As four isotopes yield consistent results, it seems to be improbable that it originates from a spurious effect. On the other hand—although highly improbable—it could in principle result from the use of an erroneous hyperfine field of RhFe for the derivation of the nuclear g factors. Thus the resonance shift data for Ni as host lattice may yield additional information. These are listed in Table IV, together with the respective data for Fe as host lattice. The ratio of the resonance shifts in Fe and Ni, which is independent of the hyperfine field, yields

$$K_{\text{Fe}} - K_{\text{Ni}} \approx \frac{1 + K_{\text{Fe}}}{1 + K_{\text{Ni}}} = -0.037(9),$$

i.e., different from zero with statistical significance. Thus the new data support again the relatively large negative Knight-shift parameter for Rh in Fe, which seems to be an exceptional case and which cannot be explained at present.

ACKNOWLEDGMENTS

We wish to thank Dr. P. Maier-Komor and E. Kellner for the preparation of the target foils, Dr. H. Schweickert and K. Assmus for the α irradiations, and E. Smolic and J. Hesol for experimental help. This work was funded by the German Federal Minister for Research and Technology (BMFT) under Contract No. 06 TM 178/I, and, partly by the Kernforschungszentrum Karlsruhe.

*Present address: EP Division, CERN, CH-1211 Geneva 23, Switzerland.

¹E. Matthias and R. J. Holliday, Phys. Rev. Lett. **17**, 897 (1966).

²R. Eder, E. Hagn, and E. Zech, Phys. Rev. C **32**, 1707 (1985).

³G. Kaendl, F. Bacon, H.-E. Mahnke, and D. A. Shirley, Phys. Rev. C **8**, 1074 (1973).

⁴E. Hagn, J. Wese, and G. Eska, Phys. Rev. C **23**, 2683 (1981).

⁵R. Eder, E. Hagn, and E. Zech (unpublished).

⁶E. Hagn and G. Eska, in *Proceedings of the International Conference on Hyperfine Interactions Studied in Nuclear Reactions and Decay*, Uppsala, Sweden, 1974, edited by E. Karlsson and R. Wäppling (Upplands Grafiska AB, Uppsala, 1974), p. 148.

⁷H. Kempter and E. Klein, Z. Phys. A **281**, 341 (1977).